Simulation of heavy-ion slowing-down tracks with the SCENA code

M. LAMOTTE[a], G. DE IZARRA[a], C. JAMMES[a]

[a] *CEA, DES, IRESNE, DER, Instrumentation Sensors and Dosimetry Laboratory, Cadarache, F-13108 Saint-Paul-lez-Durance, France.*

Abstract

In the frame of dependable neutron flux instrumentation development for Generation IV reactors, the French Atomic and Alternative Energies Commission (CEA) investigates an innovative technology based on optical signal produced within a fission chamber. In such gaseous detectors, neutrons interact with fissile material, releasing heavy ions in the MeV range, eventually leading to spontaneous photons emission in the ultraviolet to infrared range. We hereby present the space-time evolution of heavy-ion slowing-down tracks parameters in noble gases, as computed with the SCENA radiation-induced cold-plasma simulation tool. Preliminary results on excited-states noble-gas population dynamic are reported. Population of upper-lying gas levels is completed within picoseconds, only micrometers behind the projectile ionization trail.

Keywords: fission chambers, particle transport, gaseous detectors, gas scintillation

PACS: 29.85.-cAMODIF, 28.50.Dr, 28.41.Rc

---

1. Introduction

The French Atomic Energy and Alternative Energies Commission (CEA) designed a new generation of neutron detector for Gen-IV reactors flux monitoring, based on the luminescence of rare gases [1–3]. In so-called optical ionization chamber, a thin layer of neutron-sensitive material, as ^{235}U or ^{10}B is deposited on the inner detector surface, eventually releasing ions in the MeV/amu kinetic energy range upon neutron field exposure. The slowing-down of heavy-ions with a high ionization power in a rare gas —neon or argon, induces excitations and ionizations along their tracks. Spontaneous photon emissions of the excited gas atoms, in the ultraviolet to near-infrared spectrum, may be channelled in an optical fibre, to be detected by a remote solid-state photon counter. Such detectors, as CANOE (CApteur de Neutrons à Optique Expérimentale), have been successfully assessed on research reactors for proof of concept validation, sensitivity and linearity evaluation. To design, optimize and calibrate future detectors, a physics simulation of light-generating processes has to be developed. This paper starts with a historical review of radiation-induced cold-plasma simulations, their hypothesis and limitations. SCENA, our self-developed fission-induced plasma simulation code [4] is briefly described. A comparison between previous analytical work and SCENA set with similar hypothesis is assessed. Even though analogous results may be obtained by both methods with similar hypothesis, a more realistic model coupling heavy-ion and electrons transportation outputs substantially different parameters in terms of electrostatic field generation, electron energy probability function and decay times. Future developments and discussions are presented in the conclusion.

2. Methods

Theoretical investigations of radiation-induced cold-plasma, especially fission-fragments generated, have been a challenge for the past 50 years. Potential applications of such plasmas included nuclear-lasers, spaceship propulsion and optical ionization chambers for fission and fusion reactors monitoring. Several authors attempted to model these non-thermal plasma by postulating a Partial Local Thermodynamic Equilibrium (PLTE), and an established steady-state regime [5–7], finally solving a set of Boltzmann equations [8]. Electron Energy Distribution Functions (EEDF) were found to be almost a Maxwellian around thermal energies [9–11], with a low yield energy tail up to keV values. As the calculated mean energy was well below gases' inelastic reactions thresholds, the high energy part of the electron spectrum was considered responsible for metastable and excited states population [12–14]. While such hypothesis can be assumed in homogeneous low-pressure plasmas with intense energy deposition rates —as in nuclear-lasers— they however cannot be retained in a low-energy deposition rate systems having spatial heterogeneity, as noble gases excited by low rates fission fragment sources.

With respect to Optical Emission Spectroscopy (EOS) analysis of alpha-particles and fission fragment induced cold-plasmas in an analytical and a prototype optical ionization chamber, no recombination continua were detected and no emissions from ionised states of rare gases indicated very low ionisation rates, incompatible with PLTE assumptions [2].

We chose, as Budnik et al. [15] to study individual slowing down tracks mechanisms along a space and time evolution in an attempt to build future radiation-plasma macro-model, considering the plasma as an assembly of independent ionization tracks. Population states of this problem is achieved by a Monte-Carlo solved particle transport computer code developed previously, the Simulation of Collisions Electrons-Neutrals in Atmospheres (SCENA) [4]. SCENA allows a 3-dimensions and time coupled analysis of both projectile ions and delta-electrons interactions with a monoatomic buffer gas, as found in fission chambers.

2.1. Physics coupling in heavy-ion slowing-down mechanism

Typical times encountered in the generation and die-away of a heavy-ion track may differ by several orders of magnitudes, allowing uncoupled mathematical simulation of some physical processes. We hereby review main time scales of interactions mechanisms.

Fission fragments generated in a fissile coating may be released at kinetic energies up to 99 MeV, corresponding to an initial velocity of about 14E+6 m/s for an ideal Light-Fission Fragment (LFF, atomic mass = 96). Heavy ions' stopping powers, computed from HKS semi-empirical model revised by Stolterfoht [16] or from ICRU 73 tables [17, 18], input in a Continuously Slowing Down Approximation

(CSDA) solved with explicit Euler integration scheme provide an estimation of their ranges, slowing-down times and secondary-electrons energy spectra.

LFF in 1 atm neon crosses the first millimetre from emission layer's surface in 72 pico-seconds but completely transfers its kinetic energy in about 45 mm, a distance covered in 11 ns.

Energetic electrons originating from the heavy-ion/buffer gas interaction, with an average kinetic energy of about 40 to 50 eV, may ionize or excite the gas until falling below its first excitation threshold, in pico-seconds.

The similar lifetimes in a plasma sheath of heavy-ions and super-threshold secondary electrons accordingly implies necessity for a coupled simulation of both fission fragment transport and ionization tracks die-away. Conversely, thermalization of subthreshold electrons, sterile for luminescence production in the ultraviolet to near-infrared spectrum, takes significantly longer times scales, in the order of a microsecond. Such low-energy, long-lasting electrons may be discarded from the simulation if no external energy input, as an electric field, is present.

These times can be put in perspective with the tens of nanoseconds of atomic spontaneous emission and of the most probable atomic collision time in a 1 atm gas at room temperature, 1 ns (for a 1.5Å diameter Argon atom at a thermal mean velocity of 400 m/s).

2.2. Heavy-ion transport

The present section sums-up physical models implemented in SCENA for simulation of processes considered in excited levels population induced by heavy-ions-to-gas energy transfer. The following hypothesis were applied;

- A single heavy-ion is emitted in an homogeneous medium (gas) with a discrete initial energy and charge
- Heavy-ions travel in straight paths following Continuously Slowing-Down Approximation (CSDA)

- Heavy-ions only transfer energy to the gas through ionisations along their tracks, no direct-excitation is considered, neither nuclear collisions
- Heavy-ions having potential ranges of less than a millimetre are discarded from simulation
- Ejected delta electrons may ionize, excite or heat-up the gass
- No recombinations nor metastable states electron-impact de-excitations are considered

An external electric field, normal to the heavy-ion track may be applied, as this function was already implemented in SCENA to simulate standard ionisation chambers, estimate metastable states population kinetics and validate numerical models against other Boltzmann equation solvers in reference cases. Reduced fields to be found in fission chambers are well below 5 Td, thus no Lorentz-force is applied on the swift heavy-ion.

2.3. Electron generation and transport

The heavy-ion slowing-down profile in a buffer gas, subdivided in millimetre-long segments with averaged parameters such as charge, velocity or stopping-power allows uncoupled computation of optical spectra in regions of interest ie. around the emission layer, or at the end of heavy-ion track.

The Singly Differential Cross-Section (SDCS), obtained with HKS formula revised by Stolterfoht [16], calculated along each millimetre characterises the initial delta-electron emission energy spectrum and population.

During their free-flight, electrons move given the resulting Lorentz-force due to an external or the self-induced electrostatic field —if considered— and their own inertia. Excitations, ionisations and elastic collisions probabilities are computed and recorded at each random census-time —in the order of tens of femto-seconds for analysis, as well as the Electron Energy Distribution Function (EEDF).

2.4. Electrostatic field

Local electrostatic field within a heavy-ion plasma sheath is generated by charged particles production along the slowing down track. Free electrons and ions of several generations increase swarm's size, resulting in a local difference of potential, to evolve with time, gas composition and speed of seed electrons, moving substantially faster than ions.

This self-induced electrical field may shift EEDF, eventually impacting the excited gas levels population. To analytically estimate an electrostatic field around the heavy-ion track, Budnik et al. proposed the following hypothesis;

- Heavy-ion travel time is considered negligible in regard of the primary electrons die-away time
- Plasma track is cylindrical and radially symmetrical
- Ionization events do not create another generation of electrons
- No diffusion of resonance radiation are modelled
- Attachment occur if an electron is below a given distance of an atom
- Initial electrons are set along a corona after few (not considered) interactions, with a Gaussian radius distribution
- Initial electron and ion populations in helium are set to $< r_e^2 >= 4\mathtt{E}\text{-}8\ \mathrm{cm}^2$
- Energy degradation by atomic impact, molecular ion formation and recombination

The first hypothesis being questionable with respect to typical process times encountered in a plasma track calculated in Sect.2.1, will solely be implemented in SCENA for comparison purposes. A Particle In Cell (PIC) is set up to discretize a semi-infinite cylinder of 100 µm radius, representing the plasma sheath, into 50 cylindrical subshells.

To estimate the electric field inside an thin subshell of radius ranging between r and $r + dr$, with a charge density ρ_e computed by counting particles within shell's boundaries, we set-up a classical electrostatic approach.

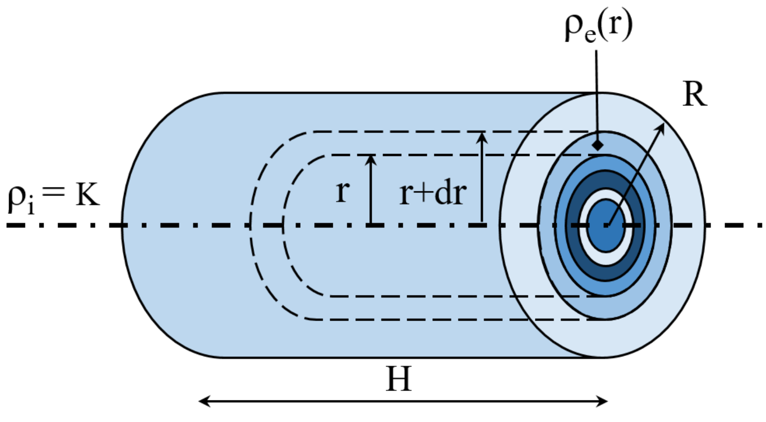

Figure 1: Electrostatic model along the heavy-ion slowing-down track of length H and radius R. Charge densities varying with respect to distance from centre of the plasma sheath is denoted $\rho_e(r)$, ion linear charge density produced by heavy-ion impact along the track is referred as ρ_i.

It is noteworthy that we considered positive ions standstill regarding their thermal motion velocity against the tens of eV of free electrons. In the picoseconds studied in our simulations, where gas may be excited by electrons, ions remain in their birth subshells.

Fig. 1 shows the electrostatic field model set in a new SCENA function to compute analytically electric field around the semi-infinite heavy-ion track. Two sets of equations define electric field generated by charges in cylindrical shells, and by gas ions along a central line. Track-length segment H of the heavy-ion being considered infinitely longer (1 mm) than its radius R, of about a micron, by applying Gauss theorem, we define:

$$\frac{\sum Q}{\varepsilon_0} = \oint \vec{E} \bullet d\vec{A} \tag{1}$$

The volume of a sheath located at radius r is simply:

$$V_s = 2\ H\ \pi\ r\ dr \tag{2}$$

electric field generated by free charges E_e at a radius r_s is:

$$\frac{\int_0^{r_s} \rho \ H \ 2 \ \pi \ r \ dr}{\varepsilon_0} = 2 \ E_e \ \pi \ r_s \ H \tag{3}$$

finally;

$$E_e(r_s) = \frac{\int_0^{r_s} \rho \ r \ dr}{\varepsilon_0 \ r_s} \tag{4}$$

Gas ionisations due solely to heavy-ion impacts generate positive charges along a linear track, inducing an electric field E_i described by Eq 5.

$$E_i(r_s) = \frac{\bar{N}_\delta}{2 \ \pi \ \varepsilon_0 \ r_s} \tag{5}$$

where $\bar{N}_\delta$ is the ionization events number on the heavy-ion track's segments, as computed by SCENA's slowing-down module.

3. Results

Results on population of excited states, their locations and Electron Energy Distribution Functions (EEDF) were computed as function of the time elapsed since departure of the projectile heavy-ion during its first millimetre journey in a buffer gas. As a matter of comparison with other authors, local electron densities, electric fields and EEDF were assessed, assuming an instantaneous transport of the projectile and a cylindrical symmetry around the semi-infinite heavy-ion trajectory, for various radius and census times, neglecting transport of the latter. All results presented below were computed with parameters to be found in a CANOE fission chamber as exploited on ORPHÉE and CABRI research reactors. Table 1 sums-up simulation inputs of our particle transport in the case of excitation produced by an ideal Heavy Fission Fragment (HFF).

Projectile	HFF
E_0 (MeV)	68
A (amu)	130
Z	54
Z_{eff_0}	13.8 [4]
Target	**Neon**
Density (cm^{-3})	2.68E+19
Temperature (K)	300
HFF-impact ionisations (first mm)	7E+4
Mean electron energy (first mm, eV)	45

Table 1: Input values for electron-slowing down simulation in a CANOE optical ionization chamber.

3.1. Evolution of secondary electrons in a semi-infinite sheath

Initial HFF-impact ionizations develop continuous distributions of electrons described by the corresponding SDCS, with an average energy —45 eV— well above neon's first ionization threshold —21.56 eV—. As depicted Fig. 2, EEDF in the centre of the plasma sheath shortly after projectile's passage is mainly composed of slow first-generation electrons produced by heavy-ion impact ionizations. At further locations, EEDF present harder spectra, consisting of fast electrons that could travel the long distance in such short time, and low-energy secondary electrons produced by fast super-threshold first-generation electrons.

Similarly, on a longer time scale, super-threshold electrons being moderated down to sub-ionization level, energy spectra reflect a swarm being mostly scattered elastically. Fast super-threshold electrons, able to produce ionizations and excitations induce a shoulder on the energy spectrum visible around 16.62 eV, neon's first excitation level. At this given time, no further increase of swarm's size is excepted and only few excitations up to lower-lying ${}^1S_x$ levels can be provoked until mitigation of electron's energy down to thermal motion.

A close-up on electron swarms at shorter distances from projectile track's

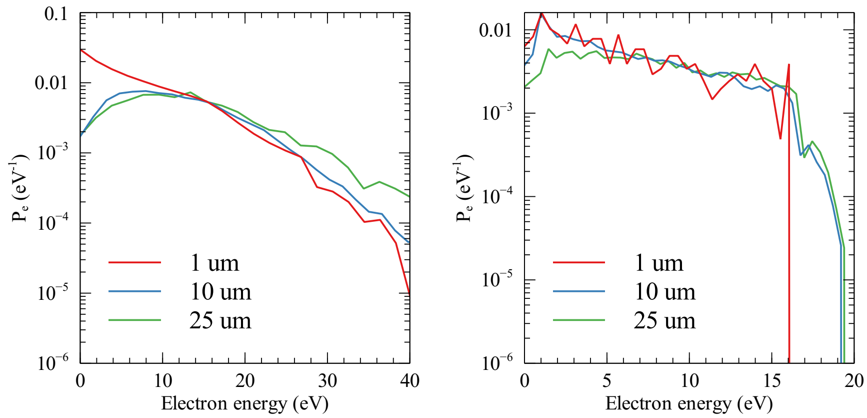

Figure 2: EEDF of electrons generated by both ion-impact and electron impact ionization on neon at 1 atm at various sheath radius, 10 ps (left) and 100 ps (right) after a projectile instantaneous passage.

centre, in the micrometre range as on Fig. 3, highlights secondary electrons emission mechanism. Initial distribution, characterized by SDCS with a tail up to keV values at HFF first millimetre, quickly falls below ionization threshold value. As super-threshold electrons may travel long distances, up to hundreds of micrometers, high energy tail remains visible for extended census times at high radius, to be shifted down to thermal energies with a delay function of inner radii.

Near the end of the heavy-ion track, where only low-energy electrons are initially emitted, expansion of the sheath takes longer time and does not contain subthreshold electrons past few micrometers, resulting in a lower gas excitation probability.

3.2. Evolution of electrostatic field a semi-infinite sheath

Electron densities around the heavy-ion track are subjected to two opposite mechanisms. Fast expansion of the swarm initially generated along a line, tends to decrease electron density as function of radius and time. On the other hand, as ionizations events occur, generation of ions and free electrons increases charge densities in some shells.

Fig. 4 presents electron densities around a HFF slowing-down track in neon, along its first millimetre, from which electrostatic field calculations have been

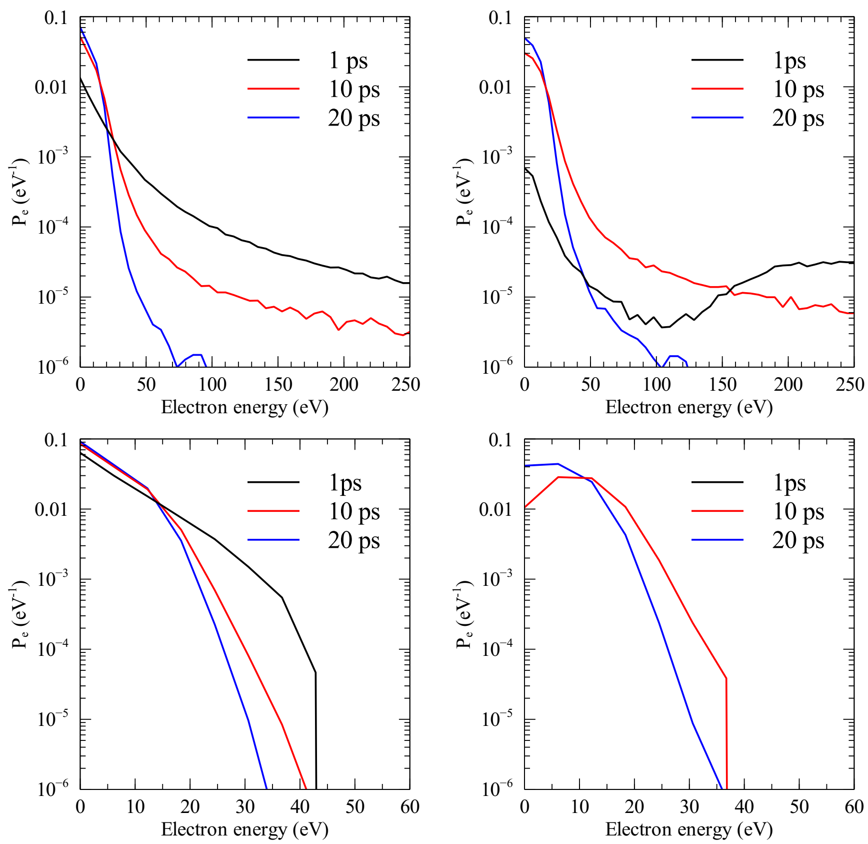

Figure 3: Up: EEDF of electrons generated by both ion-impact and electron impact ionization on neon at 1 atm at various census time, along the first mm crossed by HFF, in the shell of radius 0 to 1E-4 m (left), and 1E-5 to 1E-4 m (right).
Down: same parameter but at the last computed heavy-ion track millimetre segment, with an initial kinetic energy of 1.4MeV. No electrons had time to reach the external subshell within 1 ps.

performed.

Heavy-ions displaying higher stopping power in denser gases, associated electrostatic field substantially increases charged particles production per unit length, and so reduced electric field in the first picoseconds of the electron dying-away.

Self-induced electric-fields up to several MV/m may generate an electrostatic force, oriented radially and quickly decreasing after ion's passage. In 1 atm xenon, this electrostatic field located 0.15 µm from track's centre, 0.2 ps after ion's passage rises a local reduced field of 68 Td, resulting in a radial acceleration of 3E+17 m.s^{-2}. Despite their high values, self-induced electric forces don't induce significant changes in global EEDF and buffer gas excitation level population apportionment because of a fast decay.

3.3. Global yield and position of inelastic events

Activation of the heavy-ion time-resolved transport routine and electron seeding of SCENA allows complementary investigation of the electron swarm parameters from a more realistic point of view. In such case, new electrons with random direction vectors and initial velocity computed from SDCS are added at each simulation census-time.

Fig. 5 plots the total excitation rate of neon's level $^2P_6$ (18.64 eV) responsible for 692.95 nm line emission and $^1S_5$ lowest metastable level (16.62 eV) as function of time in the first millimetre long sheath of plasma. A maximum swarm size is obtained 112 ps after passage of the projectile. This value is coherent with the sum of time for HFF to cross the cell, 105 ps, and time for SDCS-described electron swarm to fall below neon's ionisation threshold, ∼3 ps.

In the presence of an external electric field, such as in standard fission chambers, a drift of electrons and so ionisations events' positions is noticeable, as depicted Fig. 6. If the applied reduced electric field is above breakdown voltage (about 1 Td for 1 atm neon), inelastic events keep increasing after disappearance of the projectile from the cubic-sided millimetre cell, as well as a general deviation of swarm's position from the track centre.

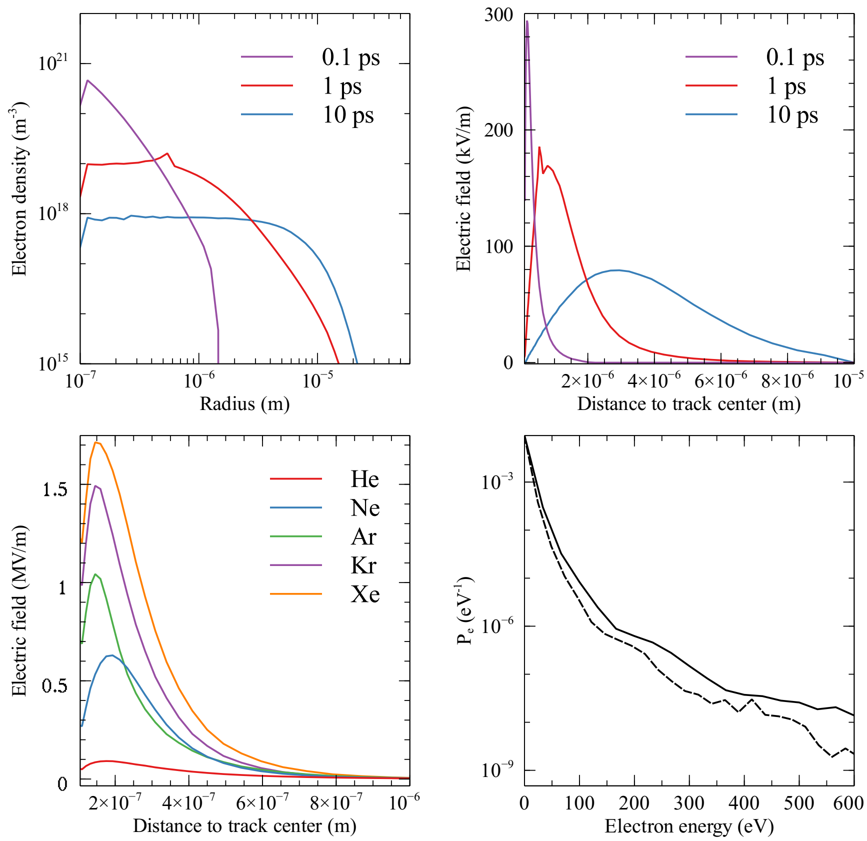

Figure 4: Up: Electron densities at various radii and census-times in 1 atm neon bombarded by HFF (left) and associated electric field (right) in the assumption of instantenous projectile journey over 1 mm.
Down: Impact of the buffer noble-gas specie on the electric field in the corona around the projectile, 0.2 ps after seed-electron release (left). EEDF in 1 atm Xe 100 ps after seed-electron release with (solid line) and without (dashed line) considering self-induced electrostatic field (right).

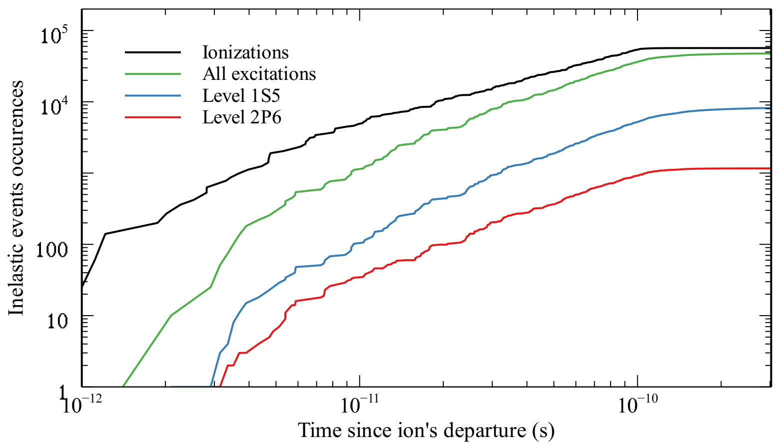

Figure 5: Evolution of accumulated excitation and ionization events of 1 atm neon by secondary HFF-induced electrons as function of time after projectile's passage.

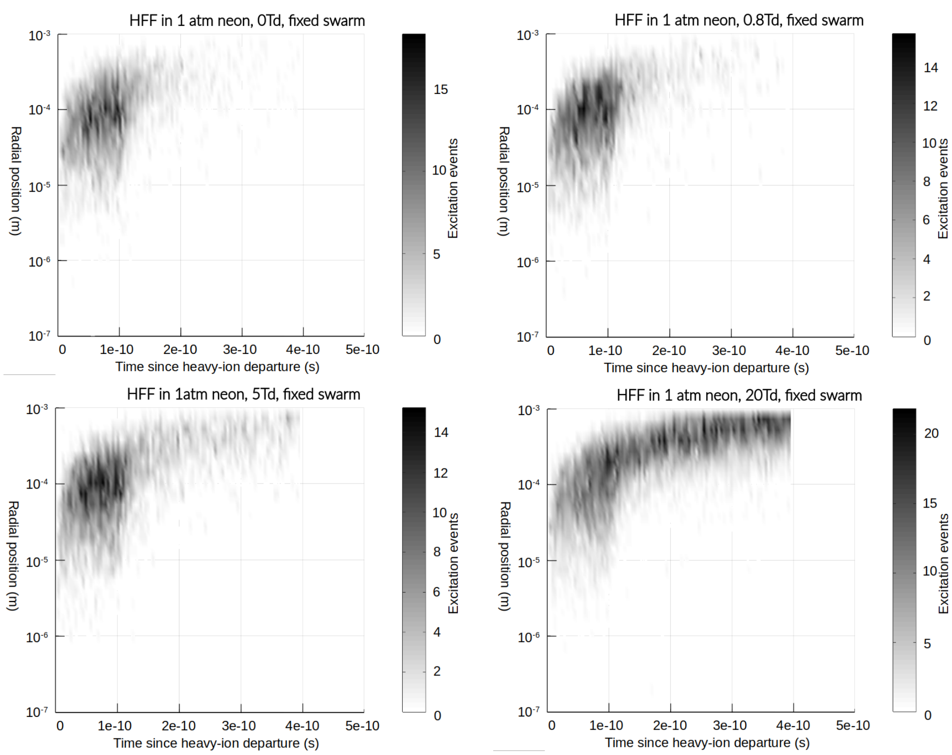

Figure 6: Radial position of excitation events from the heavy-ion track-centre in a 1 mm-sided neon cubic cell as function of time since ion's departure, in the presence of an external electric field of: up left 0 Td, up right 0.8 Td, down left 5 Td, down right 20 Td. In all cases, the HFF exits the cell after 105 ps.

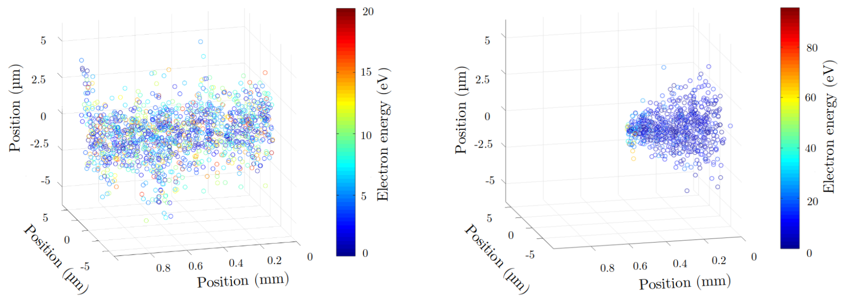

Figure 7: 3-Dimensional views of the electron swarm energy distribution (colour circles) produced after a 50 ps simulation.
Left: with instantaneous projectile transport hypothesis. Right: with coupled transportation of the HFF. In both cases, about 1000 electrons are displayed.

3.4. Space and time evolution of the global electron swarm

A 3-dimensional representation of the electron swarm generated around a HFF track, with only 1/200 th of electron population to be found in real cases is presented Fig. 7. Fast degradation of secondary electron's energy, as detailed in section 3.1 and clearly visible on 3-D views lead to an overall low EEDF over the complete plasma track. Fig. 8 shows the global EEDF of a 1 mm plasma track as function of time. Such distribution, while different from thermal motion distribution remains relatively energetic for a long time, in the order of microseconds without other diffusion mechanisms, but is sterile for further excitation level population.

Inelastic events production, useful for luminescence generation appears to be located close around the projectile heavy-ion (in micrometres radii), and mostly along the first millimetres of its track, as further steps induce low-energy deposition rates.

4. Conclusion

A simulation of heavy-ion slowing-down and energy-transfer to noble gas has been performed in configurations to be found in optical ionization chambers. Secondary electron swarms have been analysed by their space and time energy spectra evolutions. Fast degradation of electrons energy implies population of

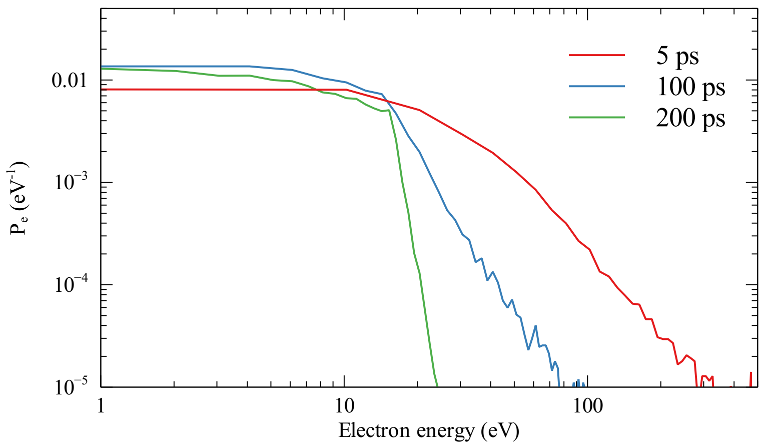

Figure 8: EEDF of electrons generated by both ion-impact and electron impact ionization on neon at 1 atm along the projectile's passage in the first 1 mm-segment. Times are given since ion departure from fissile layer. HFF is expected to leave the mm-sided cell after about 105 ps.

near-infrared emitting gas excitation levels to be complete picoseconds after heavy-ion passage, in the very first millimetres of its track, and around a radius of few micrometres. Electrostatic field and associated force generated by free flying charges around a heavy-ion track have been estimated and display values up to kV/cm in helium, and up to MV/cm in xenon, modifying slightly electron energy spectrum distribution in the corona around swift heavy-ion. Nevertheless, such narrow-located phenomenon cannot be observed in a more realistic simulation, considering swift heavy-ion time of flight as non null. Typical reaction times found within an ion-generated plasma track unveil requirement of a coupling of projectile and secondary electron swarm dynamic equations to be representative of such non-equilibrium transient plasma. Future improvements of SCENA may include collisionnal de-excitation model, as pressures in fission chambers induce atomic collision times in the order of excited-states radiative decay constants.

References

[1] M. Lamotte, G. De Izarra, C. Jammes, Development and first use of an experimental device for fission-induced spectrometry applied to neutron flux monitoring, Nuclear Instruments and Methods in Physics Research Section A: Accelerators, Spectrometers, Detectors and Associated Equipment 953 (2019) 163236.

[2] M. Lamotte, G. De Izarra, C. Jammes, Heavy-ions induced scintillation experiments, Journal of Instrumentation 14 (09) (2019) C09024.

[3] M. Lamotte, G. De Izarra, C. Jammes, Design and irradiation test of an innovative optical ionization chamber technology, Nuclear Instruments and Methods in Physics Research Section A: Accelerators, Spectrometers, Detectors and Associated Equipment 968 (2020) 163945.

[4] M. Lamotte, G. De Izarra, C. Jammes, SCENA: A simulation tool for radiation-induced gas scintillation, Nuclear Instruments and Methods in Physics Research Section A: Accelerators, Spectrometers, Detectors and Associated Equipment 982 (2020) 164576.

[5] J. Guyot, G. Miley, J. Verdeyen, Application of a two-region heavy charged particle model to noble-gas plasmas induced by nuclear radiations, Nuclear Science and Engineering 48 (4) (1972) 373–386.

[6] D. Rees, C. Leffert, D. Rose, Electron density in mixed gas plasmas generated by fission fragments, Journal of Applied Physics 40 (4) (1969) 1884–1896.

[7] J. E. Deese, H. Hassan, Analysis of nuclear induced plasmas, AIAA Journal 14 (11) (1976) 1589–1597.

[8] H. Hassan, J. E. Deese, Electron distribution function in a plasma generated by fission fragments, The Physics of Fluids 19 (12) (1976) 2005–2011.

[9] B. S. Wang, G. H. Miley, Monte Carlo simulation of radiation-induced plasmas, Nuclear Science and Engineering 52 (1) (1973) 130–141.

[10] R. H. Lo, G. H. Miley, Electron energy distribution in a helium plasma created by nuclear radiations, IEEE Transactions on Plasma Science 2 (4) (1974) 198–205.

[11] D. Auphelle, F. Euvé, M. Fitaire, A. Pointu, M. Vialle, et al., Caractéristiques électroniques d'un plasma créé par un faisceau d'ions accelerés, Physica B+ C 97 (2-3) (1979) 235–243.

[12] G. Russell, Feasibility of a nuclear laser excited by fission fragments produced in a pulsed nuclear reactor, NASA SP-236 (1971) 53–62.

[13] A. Pointu, D. Auphelle, F. Euve, M. Fitaire, M. Vialle, Calculation of the electron distribution function of a rare gas nuclear induced plasma, Journal de Physique 41 (10) (1980) 1101–1108.

[14] N. Peyraud, Energy transfer theory in particle-beam generated plasmas, Physics Letters A 106 (1-2) (1984) 37–42.

[15] A. Budnik, Y. V. Sokolov, A. Vakulovskiy, Mathematical simulation of the space-time evolution of fission-fragment plasma tracks, Hyperfine Interactions 88 (1) (1994) 185–192.

[16] N. Stolterfoht, R. D. DuBois, R. DuBois, R. D. Rivarola, Electron emission in heavy ion-atom collisions, Vol. 20, Springer Science & Business Media, 1997.

[17] P. Sigmund, R. Bimbot, H. Geissel, H. Paul, A. Schinner, ICRU - report 73, Stopping of ions heavier than helium, J. ICRU 5, 1 (2005).

[18] P. Sigmund, A. Schinner, H. Paul, Errata and addenda for IRCU report 73, Stopping of ions heavier than helium, J. ICRU 5, 1 (2009) 1–10.